4-2018

Functional Requirement for Human Pitrilysin Metallopeptidase 1 Arginine 183, Mutated in Amyloidogenic Neuropathy

Jilian E. Smith-Carpenter
Fairfield University

Benjamin Alper
Sacred Heart University

Recommended Citation

Smith-Carpenter, J. E., & Alper, B. J. (2018). Functional requirement for human pitrilysin metallopeptidase 1 arginine 183, mutated in amyloidogenic neuropathy. *Protein Science, 27*(4), 861-873. Doi:10.1002/pro.3380

THE PROTEIN SOCIETY

Functional requirement for human pitrilysin metallopeptidase 1 arginine 183, mutated in amyloidogenic neuropathy

Jillian E. Smith-Carpenter[1] and Benjamin J. Alper[2]*

[1]Department of Chemistry and Biochemistry, Fairfield University, Fairfield, Connecticut 06824
[2]Department of Chemistry, Sacred Heart University, Fairfield, Connecticut 06825

Received 13 October 2017; Accepted 29 January 2018
DOI: 10.1002/pro.3380
Published online 31 January 2018 proteinscience.org

Abstract: Here we report the enzymologic characterization of recombinant human pitrilysin metallopeptidase 1 (Pitrm1) and derivative mutants including the arginine-to-glutamine substitution mutant Pitrm1 R183Q, which has been implicated in inherited amyloidogenic neuropathy. Recombinant Pitrm1 R183Q was readily expressed in and purified from *Escherichia coli*, but was less active than the recombinant wild-type enzyme against recombinant amyloid beta-peptide (Aβ 1-40). A novel fluorogenic substrate derived from the reported Aβ 1-40 core peptide cleavage sequence, Mca-KLVFFAEDK-(Dnp)-OH, was synthesized and applied to real-time kinetic study of Pitrm1 and derivative mutants including Pitrm1 R183Q. The Pitrm1 R183Q mutant exhibited significantly decreased rate of fluorogenic peptide hydrolysis, yet retained similar binding affinity by comparison with the wild-type enzyme. Targeted mutagenic analysis revealed a functional requirement for uncharged or electropositive residues in place of Pitrm1 R183. Residue R183 is positioned within an N-terminal strand-loop-strand motif that is conserved among M16C, but not M16A or M16B family metallopeptidases. Truncation analysis revealed that this strand-loop-strand motif inclusive of residue R183 is essential Pitrm1 function. A requirement for charged residues within 4.5 Å of residue R183 was demonstrated, and Pitrm1 R183Q was found to exhibit increased sensitivity to heat inactivation. Our findings indicate that charge sharing in the vicinity of Pitrm1 R183 is critical to enzyme activity, providing potential insight into a molecular basis of Pitrm1 dysfunction.

Keywords: M16C peptidase; matrix metalloendopeptidase; presequence peptidase; amyloid beta-peptide (Aβ); neuropathy; amyloidosis

Introduction

Human pitrilysin metallopeptidase 1 (PITRM1: NCBI gene ID 10531; GENBANK reference sequence 4040225) encodes a 117 kDa metalloendopeptidase of the M16C enzyme subfamily.[1–3] Also referred to as matrix metalloendopeptidase (MP1) or mitochondrial presequence processing peptidase (PreP), the mammalian Pitrm1 gene product, localizes to the mitochondrion, where it plays a role in hydrolysis of cleaved mitochondrial targeting sequences.[4,5] In mouse models, Pitrm1 is essential to viability, as homozygous disruption causes embryonic lethality with complete penetrance.[6] Like other enzymes of the M16 family, Pitrm1 exhibits broad specificity toward short peptides that is limited in part by the requirement for potential substrates to fit into a central 13,000 cubic Angstrom binding cavity.[7,8] Notably,

Additional Supporting Information may be found in the online version of this article.

Grant sponsor: National Science Foundation; Grant number: CHE-1624774; Grant sponsor: National Institutes of Health; Grant number: 1S10RR023748-01.

*Correspondence to: Benjamin J. Alper, Department of Chemistry, Sacred Heart University, 5151 Park Ave. SC105G, Fairfield, CT 06825. E-mail: alperb@sacredheart.edu

Pitrm1 plays a role in the cleavage of amyloid beta-peptides (Aβ), the accumulation of which has been associated with amyloid neuropathy.[4,5,8–11]

A recent study of Norwegian siblings identified a recessive mutation in the PITRM1 gene (c548G > A) associated with generalized neurodevelopmental disability, spinocerebellar ataxia, mental decline, and psychosis.[11] The PITRM1 c548G > A mutation directed incorporation of single amino acid arginine-to-glutamine substitution at position R183 of the full-length derivative gene product (i.e., Pitrm1 R183Q). Pitrm1 R183Q substitution was associated with amyloidogenic neuropathic phenotype, and impaired mitochondrial function in fibroblasts isolated from siblings bearing the homozygous missense mutation.[11] Fibroblasts from the affected siblings as well as Pitrm1$^{+/-}$ mice exhibited reduced capacity to degrade Aβ peptides, and Pitrm1$^{+/-}$ mice were found to develop progressive ataxia and neurodegenerative phenotype, with accumulation of Aβ 1–42 and mitochondrial targeting signal peptides.[11]

Brunetti *et al*. observed that Pitrm1 R183Q exhibited peptide hydrolytic activity equal to or greater than that of the wild-type enzyme upon isolation of recombinant human Pitrm1 from *Escherichia coli* (*E. coli*).[11] However, Pitrm1 R183Q was unstable when expressed within immortalized patient fibroblasts, and introduction of the analogous mutation to the budding yeast homolog Cym1p (i.e., Cym1p R163Q) significantly reduced total cellular levels of the intact mutant protein which were analyzed by western blot, with evidence of increased protein degradation for the mutant homolog.[11] Accordingly, enzymologic studies of the disease-associated Pitrm1 R183Q mutant have remained limited in nature. The molecular basis of human Pitrm1 R183Q instability *in vivo* remains poorly understood, and direct functional consequences of R183Q substitution on Pitrm1 activity have not been reported.

In view of available structural data,[6,8,12–14] the Pitrm1 neuropathic R183Q substitution is positioned within a conserved N-terminal strand-loop-strand motif that is restricted to M16C, but not M16A or M16B family metallopeptidases. This motif is positioned ~10 Å distal to the enzyme active site, near an extended hinge linking N- and C-terminal enzymatic domains. Within and adjacent to the strand-loop-strand motif, several charged amino acids are positioned within 4.5 Å of residue R183. Intriguingly, the functional significance of these residues, and the enzymatic motif in which they and the disease-associated substitution are located, has not been demonstrated.

Here we investigate the molecular basis of Pitrm1 dysfunction subject to mutation of residue R183 and its structurally associated residues. We examine requirements for charge and functional group conservation using a novel fluorogenic substrate that may be of broad utility for kinetic study of enzymes catalyzing Aβ peptide hydrolysis. We observe that loss of peptide hydrolytic function is a consequence of Pirtm1 R183Q substitution and provide evidence that charge and functional group conservation among residues structurally associated with Pitrm1 R183 is critical to peptide hydrolysis.

Results

Recombinant expression, purification, and kinetic characterization of human Pitrm1 and derivative mutants

Pirtm1 and derivative mutants were expressed in and isolated from *E. coli* as C-terminal polyhistidine tagged fusion partners lacking N-terminal mitochondrial targeting sequence. Peptide hydrolytic activity was assessed using purified recombinant Aβ 1–40, and internally quenched fluorogenic peptides that included an established target of Pitrm1 activity (Substrate V), and a novel fluorogenic substrate, Mca-KLVFFAEDK(Dnp)-OH (Mca: 7-methoxycoumarin-3-carboxylic acid; Dnp: 2,4-dinitrophenyl). The Mca-KLVFFAEDK(Dnp)-OH peptide was developed for use in this study (peptide synthesis, validation, and standardization are presented in Figs. S1–S3, Supporting Information). The sequence of this peptide is centered around the core Pitrm1 cleavage site within Aβ 1–40 reported by King *et al*.[8]

Pitrm1$_{(A33\text{-}R1037)}$-6xHis (hereafter referred to as WT) and derivative mutants including the neuropathy-associated arginine-to-glutamine substitution mutant Pitrm1 R183Q were isolated as soluble proteins of the expected molecular mass [Fig. 1(A)]. As measured using purified recombinant Aβ 1–40, Pitrm1 R183Q exhibited substantially attenuated peptide hydrolytic activity relative to WT, yet retained greater activity than the catalytically inactive E107Q mutant, which served as control [Fig. 1(B, C)]. From densitometric analysis, the specific activity of R183Q mutant was about half that of the WT Pitrm1 activity toward Aβ 1–40 (3 ± 1 nmol min^{-1} mg^{-1} vs. 7 ± 1 nmol min^{-1} mg^{-1}), while the E107Q mutation essentially eliminated activity.

To investigate the mechanistic nature of Pitrm1 loss-of-function subject to introduction of the R183Q substitution, we analyzed kinetic parameters of both the wild-type enzyme and R183Q substitution mutant using novel and established fluorogenic substrates [Fig. 2(A–F)]. Pitrm1 R183Q exhibited a five-fold decrease in turnover of Substrate V, and similarly exhibited a sixfold decrease in turnover of the fluorogenic Aβ-derivative substrate Mca-KLVFFAEDK(Dnp)-OH [Fig. 2(E,F)]. Thus, by comparison with WT Pitrm1, Pitrm1 R183Q exhibited significantly decreased activity against multiple peptide substrates.

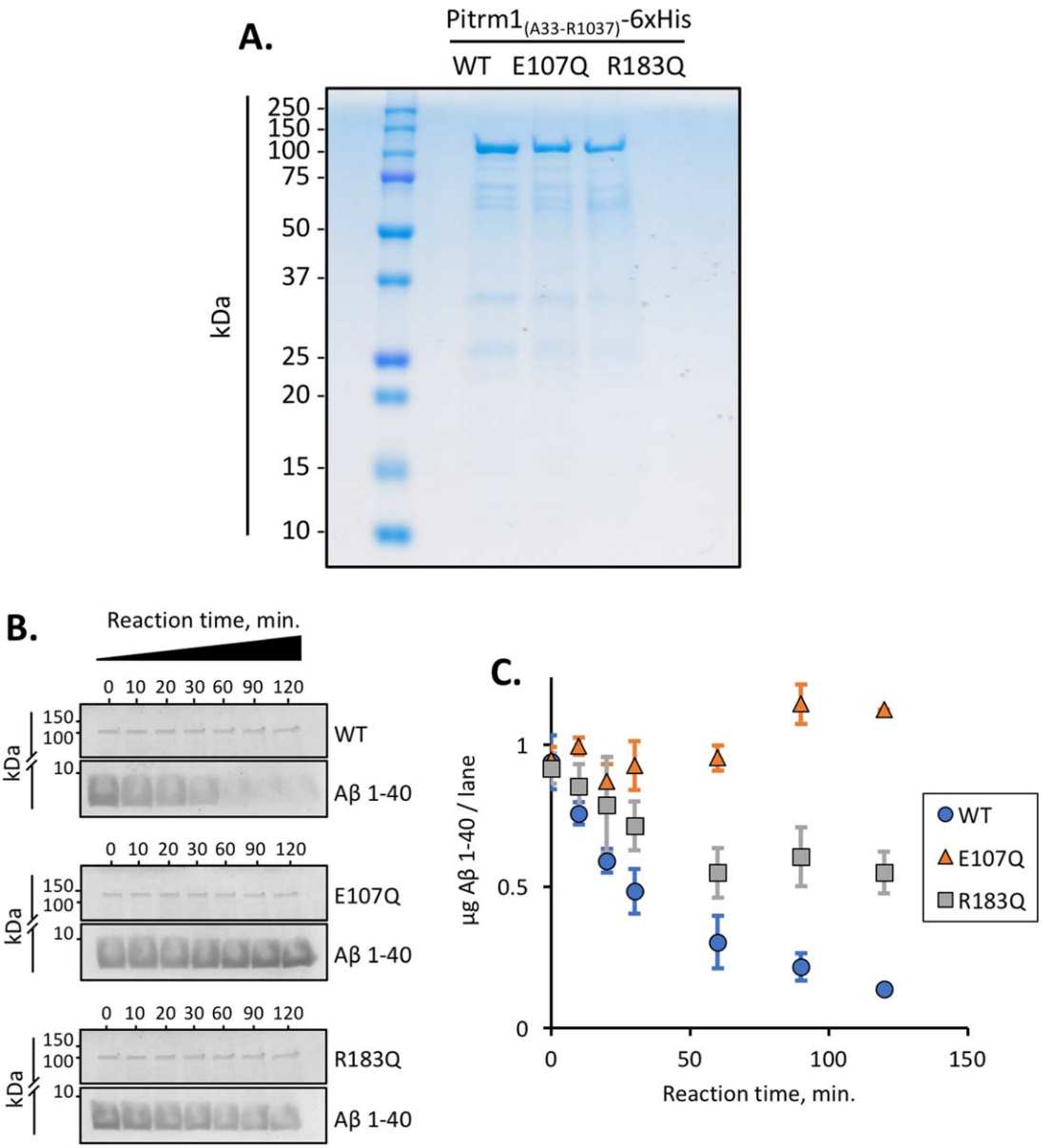

Figure 1. Recombinant human Pitrm1 R183Q exhibits partial loss of peptide hydrolytic activity towards Aβ 1–40 *in vitro*. (A) Recombinant human Pitrm1 (WT), a catalytic-site directed mutant lacking peptide hydrolytic activity (E107Q), and the human amyloid neuropathy associated substitution mutant (R183Q) were expressed in *E. coli* as C-terminal hexahistidine fusion proteins lacking N-terminal mitochondrial sequences, and purified by nickel affinity chromatography following ultrasonic cell disruption. Approximately 3 μg of each protein was separated by SDS-PAGE and visualized using Coomassie Brilliant Blue™ stain here and throughout this study. The predicted molecular mass of Pitrm1$_{(A33\text{-}R1037)}$-6xHis is 114.7 kDa. (B) Peptide hydrolysis of purified recombinant Aβ 1–40 by Pitrm1 and derivative mutants, as evaluated by SDS-PAGE. (C) Densitometric analysis of Aβ 1–40 peptide hydrolysis by Pitrm1 and derivative mutants, evaluated using BioRad ImageLab 6.0 densitometry software. Mean values ± standard error for $n = 2$ experimental replicates are shown.

We further evaluated whether reduced peptide hydrolysis activity observed subject to Pitrm1 R183Q mutation reflected decreased substrate binding affinity. For assays conducted using Substrate V, there was no difference in K_M between WT Pitrm1 and the R183Q mutant (4.7 ± 0.2 μM and 4.9 ± 0.3 μM, respectively). For assays conducted using the Aβ-derivative, the K_M for the R183Q mutant was 20% higher than WT Pitrm1 (7.6 ± 0.7 μM and 5.6 ± 0.4 μM, respectively). Peptide cleavage sites for the internally quenched fluorogenic Aβ-derivative substrate, Mca-KLVFFAEDK(Dnp)-OH, were comparable to those reported within the full-length amyloid beta-peptide[8] and were similar for both WT and R183Q mutant (Fig. S4, Supporting Information). Accordingly, reduced activity of the Pitrm1 R183Q mutant appears independent of substrate identity and may not be attributable to defective substrate binding.

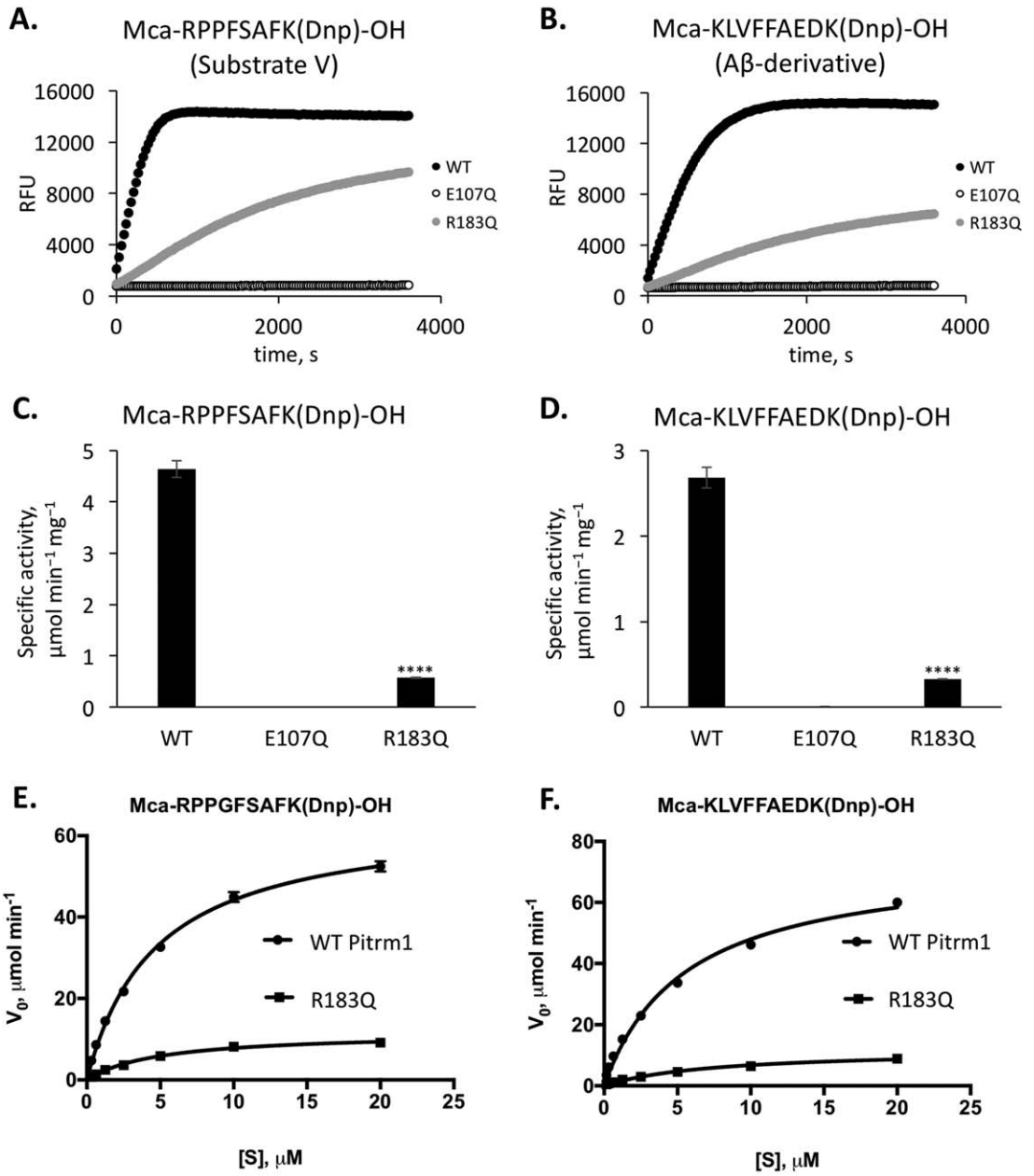

Mca-RPPGFSAFK(Dnp)-OH	WT Pitrm1	R183Q
V_{max} (μmol min^{-1})	64.8 ± 1.1	11.7 ± 0.3
K_M (μM)	4.7 ± 0.2	4.9 ± 0.3
k_{cat} (s^{-1})	6.5 ± 0.1	1.2 ± 0.1
95% CI (profile likelihood)		
V_{max} (μmol min^{-1})	62.6 to 67.1	11.1 to 12.3
K_M (μM)	4.3 to 5.1	4.3 to 5.7
k_{cat} (s^{-1})	6.3 to 6.7	1.1 to 1.2

Mca-KLVFFAEDK(Dnp)-OH	WT Pitrm1	R183Q
V_{max} (μmol min^{-1})	74.6 ± 2.1	11.9 ± 0.5
K_M (μM)	5.6 ± 0.4	7.6 ± 0.7
k_{cat} (s^{-1})	7.5 ± 0.2	1.2 ± 0.1
95% CI (profile likelihood)		
V_{max} (μmol min^{-1})	70.3 to 79.3	11.0 to 13.0
K_M (μM)	4.8 to 6.5	6.3 to 9.2
k_{cat} (s^{-1})	7.0 to 7.9	1.1 to 1.3

Figure 2. Pitrm1 R183Q exhibits lower rate of fluorogenic peptide hydrolysis, but retains similar peptide binding affinity as compared to wild-type. Kinetic parameters of peptide hydrolytic function were evaluated for purified recombinant human Pitrm1 derived from the reference gene sequence (WT Pitrm1) and subject to introduction of the Pitrm1 R183Q substitution associated with amyloid neuropathic disease (R183Q). (A) Reaction progress curves depicting sample fluorescence (RFU) as a function of time (s) for peptide hydrolysis assays conducted using Substrate V, an established target of Pitrm1 activity. (B) Reaction progress curves informing hydrolysis of Mca-KLVFFAEDK-DNP, a fluorogenic amyloid beta-peptide (Aβ) derivative. (C) Specific activity of Pitrm1, Pitrm1 E107Q, and Pitrm1 R183Q, as determined using Substrate V. Rate of peptide hydrolysis is represented in units of moles product per mole enzyme per minute, or min^{-1}. The mean values ± standard deviation for $n = 3$ experimental replicates are shown here and throughout the remainder of this study except where stated otherwise. ****$P < 0.001$ (extremely significant). (D) Specific activity of Pitrm1, Pitrm1 E107Q, and Pitrm1 R183Q, as determined using the Mca-KLVFFAEDK-DNP Aβ-derivative peptide. (E) Kinetic parameters for hydrolysis of Substrate V, Mca-RPPGFSAFK(Dnp)-OH. (F) Kinetic parameters for hydrolysis of the Aβ derivative peptide Mca-KLVFFAEDK(Dnp)-OH. Reported K_M and V_{max} values were determined by nonlinear regression analysis using GraphPad Prism™. Error bars that wholly overlap representation of the experimental data have been omitted for clarity.

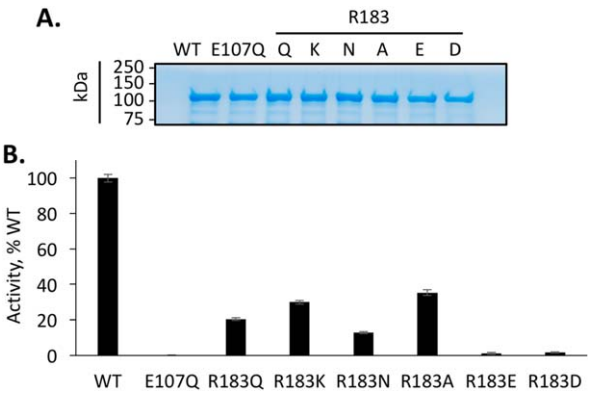

Figure 3. Mutational analysis reveals functional requirement for electropositive or uncharged residues in place of Pitrm1 R183. (A) SDS-PAGE analysis of purified recombinant human Pitrm1 R183 substitution mutants. Recombinant human Pitrm1 (WT), a catalytic-site directed mutant lacking peptide hydrolytic activity (E107Q), and targeted amino acid substitution mutants replacing native Pitrm residue R183 with lysine, asparagine, alanine, glutamate, or aspartate (R183Q, K, N, A, E, and D mutants, respectively) were purified from *E. coli* as C-terminal hexahistidine fusion proteins lacking N-terminal mitochondrial sequences. (B) Relative specific activity of Pitrm1, Pitrm1 E107Q, and Pitrm1 R183-mediated hydrolysis of Mca-KLVFFAEDK(Dnp)-OH.

Functional conservation of Pitrm1 R183 and structurally associated residues is critical for peptide hydrolysis

To inform the structural basis of reduced peptide hydrolysis activity observed subject to Pitrm1 R183 substitution, we conducted an extended mutagenic analysis of residue 183 (Fig. 3). Requirements for conservation of charge, size, and polarity at this position were evaluated through kinetic analysis of Pitrm1 R183Q, K, N, A, E, and D substitution mutants using the Aβ-derivative substrate Mca-KLVFFAEDK(Dnp)-OH [Fig. 3(B)]. All tested substitution mutants of residue 183 were isolated as highly enriched proteins of the expected molecular mass [Fig. 3(A)]. The identity of residue 183 was critical to Pitrm1 activity, as only substitutions that retained positively charged or uncharged residues in position 183 were well tolerated. Of the mutants characterized, only R183K and R183A retained greater than 20% of WT activity.

Pitrm1 R183 is positioned within a strand-loop-strand motif of the N-terminus that is directly exterior to the catalytic Zn^{2+} ion, comprising amino acid residues W182-K199 (Fig. 4). This motif links two adjacent alpha helices that are positioned adjacent the region of defined electron density for Aβ 1–40 within the substrate bound crystal structure and is itself positioned under and adjacent to an extended helical hairpin or hinge (amino acids 510–575), which serves to connect the N- and C-terminal enzymatic domains. The strand-loop-strand motif incorporating residue R183 is structurally conserved among M16A, but not M16B or M16C peptidases, and is bounded at either end by glycine residues positioned about 10 Å from the catalytic zinc ion. Within this motif, residue R183 is positioned about 14 Å from the catalytic zinc ion [structural perspectives are presented in Fig. 4(A–C)].

To evaluate the contribution of the strand-loop-strand motif comprising residues W182-K199 in Pitrm1 activity, we engineered a truncation mutant bearing full deletion of this region (i.e., Pitrm1 Δ182–199). The Pitrm1 Δ182–199 truncation mutant was isolated as a single molecular weight species of the expected molecular mass [Fig. 4(D)], yet did not exhibit detectable peptide hydrolytic activity against the Aβ-derivative substrate Mca-KLVFFAEDK(Dnp)-OH [Fig. 4(E)], indicating an essential role for residues of this motif in peptide hydrolysis.

Requirement for charge and functional group conservation in proximity to Pitrm1 R183

The strand-loop-strand motif comprising residues W182-K199 and structurally proximate region of the Pitrm C-terminus contain several conserved charged residues within potential ionic bonding distance of Pitrm1 residue R183 [Fig. 5(A)]. For example, residues E185, K199, K901, and E902 are positioned within 4.5 Å of R183 within the crystal structure of Pitrm1 in complex with Aβ 1–40.[8] To assess the role of these residues in Pitrm1 function, we engineered charge substitution mutants introducing amino acids with R-groups bearing charges complementary to the native enzymatic residues (i.e., E185R, K199E, K901E, and E902R substitution mutants). Substitution mutants were isolated as highly enriched proteins of the expected molecular mass, and all mutations had at least some impact on activity [Fig. 5(B,C)]. Intriguingly, the greatest impact on peptide hydrolytic activity was observed for charge substitutions introduced in place of residues of the strand-loop-strand motif. E185R and K199E substitution mutants retained less than 20% of WT activity, compared with greater than 40% retained activity for substitutions K901E and E902R, supporting an important role for charge conservation among residues of the Pitrm1 strand-loop-strand motif adjacent to residue R183 in enzymatic function.

We next sought to define charge, polarity, and functional group requirements in Pitrm1 R183-adjacent residues E185 and K199, by examining the role of these residues in enzyme activity (Fig. 6). E185D, N, Q, A, K and R, and K199R, A, Q, N, D, and E substitution mutants were constructed, and their peptide hydrolytic activity was evaluated using the Aβ-derivative substrate Mca-KLVFFAEDK(Dnp)-OH. In place of native residue E185, conservation of electronegative or polar uncharged amino acids containing side-chain carbonyl groups was important for Pitrm1 function. E185D, N, and Q substitution

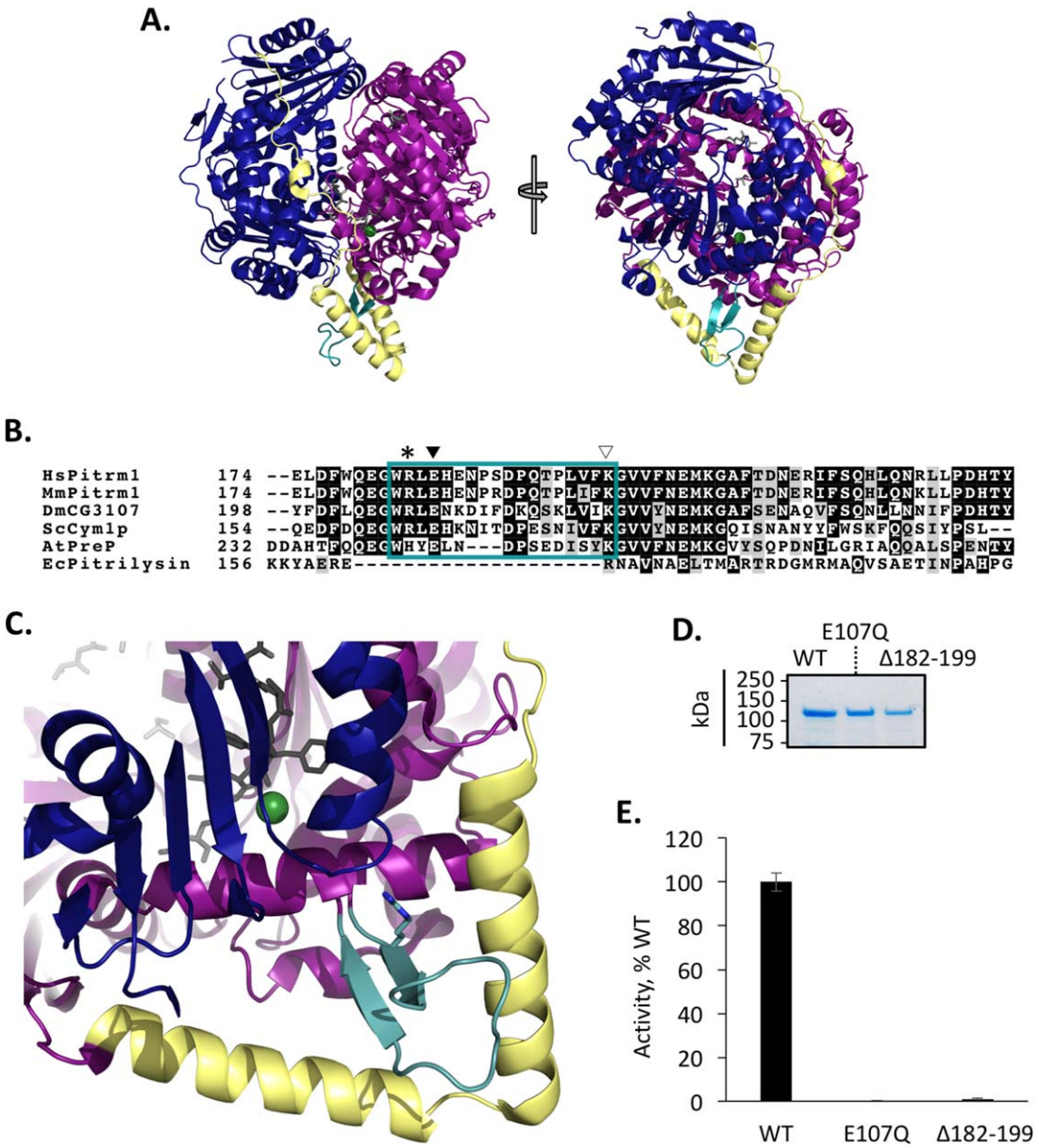

Figure 4. Strand-loop-strand residues W182-K199 are essential for Pitrm1 activity. (A) Structural model of human Pitrm1 (hPreP, RCSB PDB# 4NGE) retaining orientation and coloring conventions of King *et al*.[8] The conserved-strand-loop strand motif of M16C peptidases comprising residues W182-K199 identified in the current study has been colored deep teal. Pitrm1 N-terminal residues 33–509 are colored purple, and C-terminal residues 576–1037 are colored deep blue. N- and C-terminal domains are linked by an extended helical hairpin (yellow), which is positioned structurally adjacent to the conserved-strand-loop strand motif. Bound Aβ (1–40) is represented in gray, while the catalytic zinc ion is colored in green. Enzyme, peptide, and zinc are presented in cartoon, stick, and sphere format, respectively. (B) Primary sequence alignment of human Pitrm1 and homologs of the M16C and M16A peptidase subfamilies. HsPitrm1 residue R183 is indicated by an asterisk (*). HsPitrm1 E185 is indicated by a filled arrow (▼), and of HsPitrm1 K199 is indicated by an open arrow (▽). HsPitrm1 residues W182-K199 make up a strand-loop-strand motif restricted to M16C peptidases, indicated by a teal box with solid color outline. (C) Alternative perspective image from PDB# 4NGE showing the position of Pitrm1 residue R183 in structural context (residue R183 is represented in deep teal sticks, with nitrogen atoms colored in blue). (D) SDS-PAGE analysis of purified recombinant human Pitrm, Pitrm1 E107Q, and a truncation mutant (Δ182–199) bearing internal deletion of Pitrm1 residues W182-K199. (E) Relative activity of Mca-KLVFFAEDK(Dnp)-OH peptide hydrolysis by Pitrm1, Pitrm1 E107Q, and Pitrm1Δ182–199.

mutants retained greater than 45% of WT activity, compared with less than 20% activity for E185A, K, and R substitution mutants [Fig. 6(A)]. In place of native residue K199, conservation of electropositive or polar uncharged amino acids containing side-chain amine groups was important for Pitrm1 function, as K199R and N substitution mutants retained greater than 85% of WT activity, compared with less than 20% activity for K199A, Q, E, and D substitution mutants [Fig. 6(B)]. Thus, conservation of charge and polarity

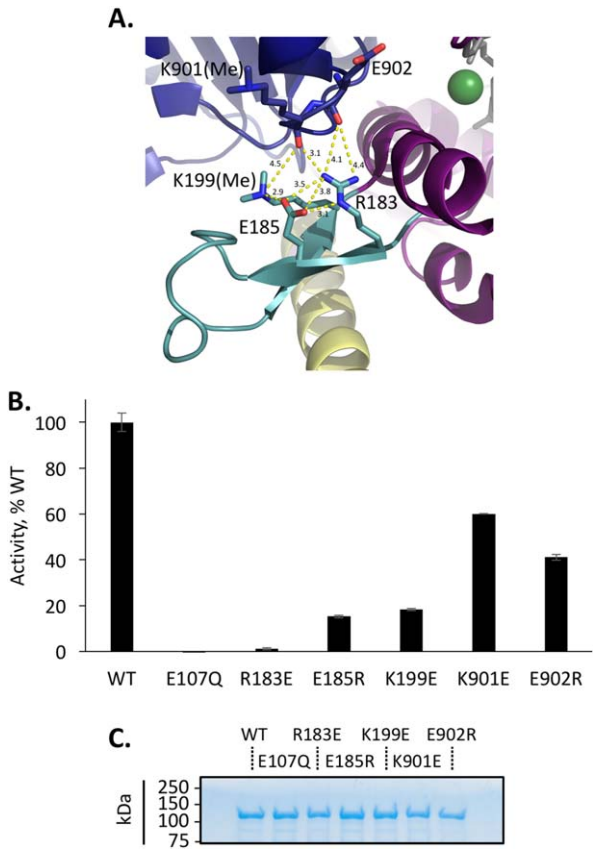

Figure 5. Charge identity of residues proximal to Pitrm1 R183 is important for catalytic function. (A) Putative complementary charge interactions within 4.5 Å of Pitrm1 residue R183 (yellow dashed lines). Residue numbers and distances of separation are indicated. An obscuring segment of the extended helical hairpin (yellow) has been removed for clarity. Surface lysine methylation was reported to facilitate crystallization but reduce catalytic activity[8] and may not reflect the native state of the enzyme. (B) Specific activity of Mca-KLVFFAEDK(Dnp)-OH peptide hydrolysis by Pitrm1, Pitrm1 E107Q, R183E, E183R, K199E, K901E, and E902R mutants. (C) SDS-PAGE analysis of purified recombinant human Pitrm, Pitrm1 E107Q, and mutants bearing of charge substitutions in place of Pitrm1 R183 (R183E), or within 4.5 Å of this residue (E185R, K199E, K901E, and E902R).

of residues E185 and K199, which are positioned within potential ionic binding distance of residue R183, appears critical for Pitrm1 activity.

To evaluate whether charge sharing between residues E185 and K199 might contribute to Pitrm1 activity, we introduced reciprocal charge substitution mutations in these residues alone and subject to additive R183Q mutation [Fig. 6(C)]. All single-site and double mutation substitutions targeting residues E185 and K199 were isolated as highly enriched proteins of the expected molecular mass [Fig. 6(D–F)]. Intriguingly, reciprocal charge reversal of residues E185 and K199 (i.e., E185R/K199E double mutation) increased Pitrm1 catalytic activity relative to that of either mutation alone, while additive R183Q substitution in the context of either the E185 or K199 mutation (i.e., in R183Q/E185R and R183Q/K199E double mutants) was more detrimental to catalytic activity. In view of these experiments, charge sharing by residues E185R and K199E appears important for Pitrm1 catalytic activity and may be influenced by residue R183 identity.

Pitrm1 R183Q substitution increases enzyme thermosensitivity

To investigate whether thermosensitivity of Pitrm1 was increased subject to introduction of R183Q mutation, we evaluated catalytic activity following heat treatment at ambient temperatures ranging from 37 to 57°C (Fig. 7). Consistent with the hypothesis that electrostatic interactions formed in proximity to residue R183 are important for Pitrm1 stability, the Pitrm1 R183Q mutant was significantly more sensitive to heat inactivation than the recombinant WT enzyme. For WT Pitrm1, half-maximal activity was observed subject to heat treatment at ambient temperature of ~49°C, significantly higher than the 42°C heat treatment temperature required for half-inactivation the Pitrm1 R183Q mutant (Fig. 7).

Discussion

Pitrm1 residue R183 is located within an essential structural motif that is conserved among enzymes of the M16C subfamily. The conserved identity of residue R183, and more broadly, conservation of the N-terminal strand-loop-strand motif in which this and other charged residues are located, is critical to Pitrm1-mediated peptide hydrolysis. In the context of this study, Pitrm1 R183Q substitution decreased Pitrm1 activity in a manner that was independent of substrate binding affinity or substrate identity and did not appear to influence major sites of peptide cleavage. Functional requirements for residues R183, E185, and K199 were demonstrated, indicating that electrostatic interactions formed in proximity to Pitrm1 R183 are critically dependent on residue identity.

The observed reduction of peptide hydrolytic activity subject to Pitrm1 R183Q substitution is in contrast with a prior report (Ref. 11; with expression and purification further described in Ref. 15). Variability in the reported and observed activity of the recombinant R183Q mutant may be attributable to differences in bacterial host genotype, protein expression construct, cell lysis, and purification methods, or another conditional difference in the experimental system that is not resolved here.

At least two potentially significant differences in experimental design differentiate our work from that of Brunetti *et al.*[11] First, the expression vector used by Brunetti *et al.*[11] directed expression of an N-terminally affinity tagged protein bearing deletion of

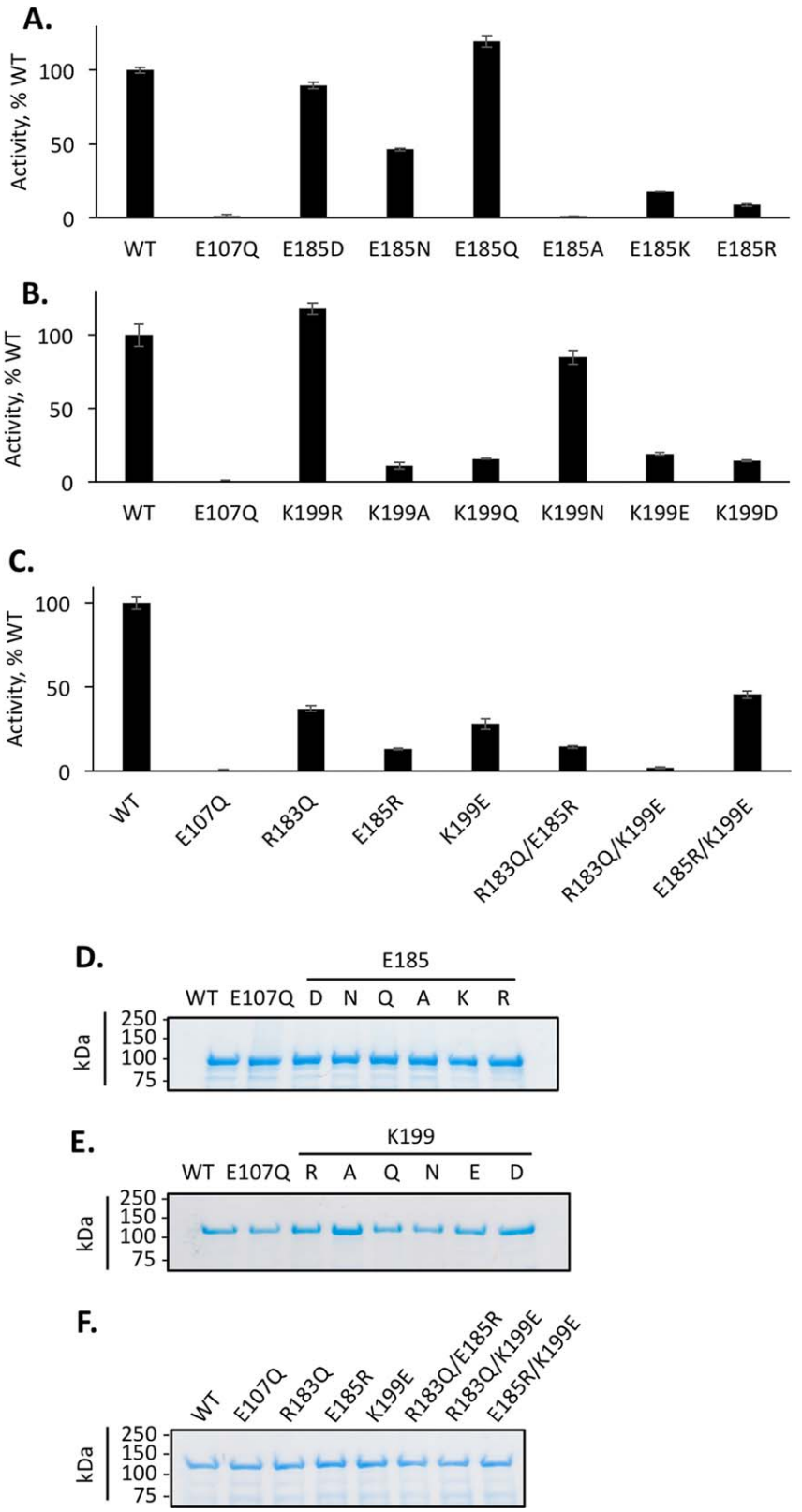

Figure 6. Charge sharing by residues E185 and K199 contributes to Pitrm1 activity and may be disrupted subject to R183Q mutation. (A–C) Relative activity of Mca-KLVFFAEDK(Dnp)-OH peptide hydrolysis by Pitrm1, Pitrm1 E107Q, and other targeted substitution mutants, as indicated. (D–F) SDS-PAGE analysis of purified recombinant human Pitrm, Pitrm1 E107Q, and other mutants.

the mitochondrial targeting sequence (i.e., 6xHis-Pitrm1Δ1–28), which differs in placement from the C-terminal polyhistidine tag appended to the truncated enzyme (i.e., Pitrm1$_{(A33\text{-}R1037)}$-6xHis) used in this study. Second, the method of cell lysis (enzymatic digestion with lysozyme vs. mechanical cell

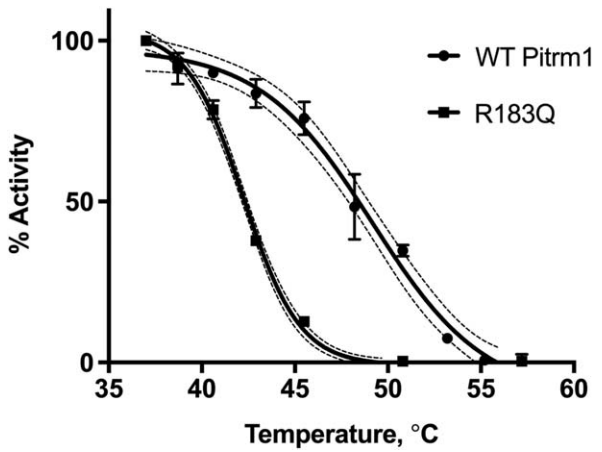

Figure 7. Pitrm1 R183Q substitution increases sensitivity to thermal inactivation. Relative activity of Mca-KLVFFAEDK(Dnp)-OH peptide hydrolysis by Pitrm1 and Pitrm1 R183Q was determined by fluorescence assay at 37°C following 3 min pretreatment at the temperatures indicated in the figure legend. Lines of best fit (solid black) and the limits of their 95% confidence intervals (dashed lines) were determined through nonlinear regression using the sigmoidal interpolation function of GraphPad Prism™ for $n = 2$ experimental replicates. As determined from interpolation of the line of best fit, 50% inactivation occurred at 49 ± 1°C for WT Pitrm1, versus 42 ± 1°C for the Pitrm1 R183Q mutant (mean values ± limits of 95% confidence interval).

disruption by sonication, respectively) differs between the two studies. Notwithstanding these differences, the WT enzymatic preparation used in this study retains comparable activity to the enzymatic preparations of Brunetti *et al.*,[11] and also to that of Teixeira *et al.*,[15] which is cited as the basis for the purification method used by Brunetti *et al.*[11]

In the current study, available evidence from size-exclusion chromatography coupled with multi-angle laser light scattering analysis (SEC-MALS; Fig. S5, Supporting Information) indicates the protein preparations are uniform, and that purified Pitrm1 and derivative mutants are of the expected molecular size. As determined by SEC, the major portion of each immobilized metal affinity purified protein preparation, representing 92–88% by mass of each purified sample, exhibited mobility between that of the 156 and 66 kDa MW size standards. For these products, MALS indicated an absolute molecular mass of ~110 kDa, which is consistent with the predicted mass of monomeric Pitrm1 (114.7 kDa). We cannot rule out localized defects of protein structure, or even broad conformational defects that are not immediately evident from this analysis. Yet, the reported expression and purification method clearly demonstrates that conservation of Pitrm1 R183 and surrounding residues is important for enzyme activity and will allow future studies that continue to explore the importance of the R183Q mutation.

Intriguingly, the reduction in Pitrm1 R183Q activity under conditions of this study suggests that the molecular basis of Pitrm1 R183Q dysfunction can be studied *in vitro* using recombinant enzymes derived from bacterial expression systems, using fluorogenic substrates such as the Aβ-derivative peptide developed and reported here. Our observation of reduced Pitrm1 activity subject to R183Q substitution thus indicates that Pitrm1 R183Q dependent dysfunction is not solely attributable to disruption of post-translational modifications that are restricted to higher eukaryotes. Moreover, as peptide binding affinities and cleavage sites appear broadly unaffected by introduction of the R183Q substitution, a direct mechanistic role for Pitrm1 residue R183 in substrate binding is not supported by our data. Rather, a model in which charge sharing by residues near Pitrm1 R183 contributes to enzyme stability or functional integrity of the enzyme active site is consistent with the increased thermosensitivity of the Pitrm1 R183Q mutant and requirements for charge conservation among nearby residues *in vitro* and is also consistent with reports of reduced stability of the Pitrm1 R183Q mutant in higher eukaryotes.[11]

We therefore conclude that structural and electrostatic properties of the conserved strand-loop-strand motif containing Pitrm1 residue R183, and indeed the identity of residue R183 itself, are critically important for Pitrm1 function. Mutational disruption of electrostatic interactions in proximity of Pitrm1 residue R183 contributes to the loss of enzyme activity observed in this study, and by extension, may contribute to the loss-of-function phenotype observed in Pitrm1 R183Q-dependent neuropathy.

Materials and Methods

Cloning, expression, and purification of human Pitrm1 and derivative mutants

The human PITRM1 gene used in this study was obtained from the GE Dharmacon™ cDNA library (GE Health Care Life Sciences, Marlborough, MA; product #MHS6278–202830697; GENBANK reference sequence 4040225).[16,17] To facilitate bacterial expression of the derivative gene product, PITRM1 was inserted from 5′ to 3′ at Nde1 and Xho1 cloning sites, respectively, within the pET-30b(+) expression vector (Novagen, Hornsby Westfield, NSW, Australia). Plasmid constructs were engineered to direct expression of a C-terminal hexahistidine fusion protein lacking the N-terminal mitochondrial targeting sequence of the proenzyme (i.e., $Pitrm1_{(A33\text{-}R1037)}$-6xHis).

Derivative mutations in PITRM1 were introduced by circular PCR amplification of the WT expression construct using mutagenic oligonucleotides (Table S1, Supporting Information), applied in

conjunction with the In-Fusion® HD cloning kit (Takara Bio USA, Ann Arbor, MI). Constructs directing expression of WT Pitrm1 and Pitrm1 R183Q were validated by DNA sequencing throughout the full open reading frame, while other clones were validated across the site of mutation or truncation only (Yale University Keck DNA sequencing facility, New Haven, CT).

Bacterial cells (strain BL21 DE3, genotype *F– ompT gal dcm lon hsdSB*(*rB- mB-*) *λ*(*DE3* [*lacI lacUV5-T7 gene 1 ind1 sam7 nin5*]), Novagen) expressing $Pitrm1_{(A33\text{-}R1037)}$-6xHis or derivative mutants were cultured in lysogeny broth under antibiotic selection with kanamycin, and induced for protein expression using 0.1 m*M* isopropyl β-D-1 thiogalactopyranoside (IPTG). Following induction of protein expression, cultured cells were grown overnight at 25°C, harvested by centrifugation (3200*g*, 20 min at 4°C), rinsed with phosphate buffered saline, and stored at −80°C prior to cell lysis. On thawing, cell pellets were lysed by ultrasonic disruption in a lysis/binding/wash buffer containing 300 m*M* sodium chloride, 50 m*M* sodium phosphate, and 10 m*M* imidazole, pH 7.4, and clarified by centrifugation (3200*g* for 15 min at 4°C). Clarified lysates were purified by immobilized nickel affinity chromatography rinsing with ∼100 column volumes of binding/wash, and eluting in an equivalent buffer supplemented to 300 m*M* imidazole. Protein concentration was determined by Bradford using against bovine serum albumin (BSA) standards. Proteins were stored at −80°C in elution buffer supplemented with 50% glycerol.

Aβ 1–40 peptide hydrolysis assays

Amyloid beta-peptide peptide hydrolysis assays were conducted using purified recombinant Pitrm1 and derivative mutants (described above), and HFIP-treated purified recombinant Aβ 1–40 (rPeptide, Bogart, GA). The 80 μL assay mixtures contained 0.85 μ*M* Pitrm1 and 50 μ*M* Aβ 1–40 in 50 m*M* potassium phosphate, pH 7.0. Enzyme and substrate premixtures were separately prepared as 2× stocks, prewarmed to 37°C, and then mixed in equal proportion to initiate the peptide hydrolysis assay. Substrate premixtures were sonicated for 5 min at room temperature prior to warming and initiation of peptide hydrolysis.

Following assembly of the peptide hydrolysis assay mixture, enzymatic reactions were quenched at 0, 10, 20, 30, 60, 90, and 120 min intervals by transfer of 5 μL of the assembled reaction mixture to 10 μL of SDS-PAGE sample buffer supplemented with EDTA (400 m*M* Tris pH 6.8, 25% glycerol, 3% SDS, 0.005% [w/v] bromophenol blue and 8% β-mercaptoethanol, 100 m*M* EDTA). Quenched samples were held on ice for the duration of the peptide hydrolysis assay and then treated at 95°C for 3 min to ensure complete denaturation prior to SDS-PAGE. Electrophoretic separation was performed using Bio-Rad Mini-PROTEAN TGX any kD 15 well gels, with protein separation performed at 150 V for 40 min in Tris/Glycine SDS buffer system provided by the manufacturer (Bio-Rad Laboratories; Hercules, CA). Following separation, gels were stained using colloidal Coomassie Brilliant Blue G250™ in accordance with the method of Candiano *et al.*[18] Densitometric measurements were obtained using the Bio-Rad Image Lab software version 6.0. Band intensity was related to abundance of Aβ 1–40 using a series of internal standards.

Mca-KLVFFAEDK(Dnp)-OH peptide synthesis and validation

Mca-KLVFFAEDK(Dnp)-OH was synthesized using standard FMOC/HBTU chemistry with an FMOC Lys(Dnp) Wang resin on a PS3 peptide synthesizer (Gyros Protein Technologies, Tucson, AZ). FMOC deprotection was completed using 20% piperidine. Each amino acid coupling was performed using 0.4 mmol FMOC protected amino acid, 0.4 mmol 2-(1*H*-benzotriazole-1-yl)-1,1,3,3-tetramethyluronium hexafluorophosphate (HBTU), and 0.4*M* N-methylmorpholine in dimethylformamide (DMF). After final FMOC deprotection, the resin was transferred to a 10 mL filtered syringe (Torviq, Tuczon, AZ) and the N-terminus was derivatized with 7-methoxycoumarin-3-carboxylic acid by double coupling with 4 eq. of the coumarin, 4 eq. of HBTU, and 10 eq. of *N*,*N*-diisopropylethylamine (DIEA) in DMF. The first coupling was shaken at room temperature for 2 h and then the resin was washed with DMF before the second coupling, which proceeded for 12 h. Resin was then washed with DMF and dichloromethane (DCM) and dried in a vacuum desiccator.

The peptide was cleaved from the resin with 10 mL of the cleavage cocktail, containing trifluoroacetic acid (TFA) (90% v/v), thioanisole (5% v/v), ethanedithiol (3% v/v), and anisole (2% v/v), for 3 h at room temperature. The peptide was precipitated by adding the cleavage solution dropwise into cold diethylether, then centrifuged to a pellet. The peptide pellet was then washed with diethylether and centrifuged two additional times. The peptide was purified by reverse-phase HPLC (Shimadzu Prominence, Shimadzu Scientific Instruments, Columbia, MD) with a Phenomenex Aeris Peptide C-18 semi-preparative column (150 × 10 mm; Phenomenex, Torrence, CA) using a 3 mL/min flow rate and a linear gradient of 40–70% acetonitrile over 15 min. The peptide was collected, frozen, and lyophilized to yield a peptide powder. The peptide product mass was confirmed by MALDI-TOF on a Shimadzu Axima Confidence mass spectrometer using 2,5-dihydroxybenzoic acid (DHB) as matrix. FMOC Lys(Dnp)

Wang resin was purchased from Anaspec (Freemont, CA) and 7-methoxycoumarin-3-carboxylic acid was purchased from Chemodex (St. Gallen, Switzerland). The FMOC protected amino acids, HBTU, deprotection solution, activating reagent, TFA, DMF, and DCM were purchased from Gyros Protein Technologies. All other reagents were purchased from Fisher Scientific. (Waltham, MA).

FRET assays for Pitrm1 activity

To better assess the impact of Pitrm1 R183Q substitution on peptide hydrolysis activity, novel and established fluorogenic substrates were employed. Substrate V (7-methoxycoumarin-4-yl-acetyl-RPPGFSAFK-2,4-dinitrophenyl, R&D Systems, Minneapolis, MN), an established Pitrm1 substrate, was used much as previously described.[4,7] For determination of specific activity, assembled 50 μL assay mixtures contained 2 n*M* Pitrm1 and 10 μ*M* initial concentration of fluorescent substrate in 50 m*M* potassium phosphate, pH 7.0. Enzyme and substrate premixtures were separately prepared and prewarmed to 37°C and then mixed to initiate the peptide hydrolysis assay directly prior to analysis. For studies of Pitrm1 thermosensitivity, enzymatic samples were incubated for 3 min at temperatures ranging from 37 to 57°C using the gradient functionality of an Eppendorf Mastercycler® PCR thermocycler (Eppendorf, Westbury, NY). On initiation of the enzymatic assay, sample fluorescence was measured at 37°C in 96-well plate format using a BioTek Synergy HT plate reader (excitation: 325 ± 25 nm, emission: 420 ± 25 nm, BioTek U.S., Winooski, VT).

To examine whether functional consequences of Pitrm1 R183Q substitution were substrate-dependent, we synthesized an internally quenched fluorogenic substrate approximating the primary Pitrm1 cleavage site in the core amyloidogenic segment of the Aβ peptide (i.e., 7-methoxycoumarin-4-yl-acetyl-KLVFFAEDK-2,4-dinitrophenyl). The peptide sequence of this substrate reflects the region inclusive of and directly surrounding Aβ 1–40 residue F20, which is positioned directly adjacent the primary scissile peptide bond in the bound crystal structure (i.e., in the P1 position[8]). Aβ-derivative substrate premixtures were sonicated for 5 min at room temperature prior to warming and input to the kinetic assay. Quantitative standardization for Mca-KLVFFAEDK-(Dnp)-OH was based on fluorescence yield of the hydrolyzed substrate by comparison with Substrate V. Kinetic parameters were determined by nonlinear regression analysis using the Michaelis–Menten functionality of GraphPad Prism 7 (GraphPad Software, La Jolla, CA). For all data, average values from $n = 3$ experimental replicates are depicted ± standard error of the mean.

Protein structure and homology modeling

Primary sequence comparisons of Pitrm1 homologs were generated using default settings of the Clustal Omega Multiple Sequence Alignment tool (http://www.ebi.ac.uk/Tools/msa/clustalo/).[19–21] NCBI curated reference sequences were input for alignment as follows: HsPitrm1: NP_001229236.1| presequence protease, mitochondrial isoform 1 precursor [Homo sapiens], MmPitrm1: NP_660113.1| presequence protease, mitochondrial precursor [*Mus musculus*], DmCG3107: NP_610156.1| CG3107, isoform A [*Drosophila melanogaster*], NP_010718.1| ScCym1p: [*Saccharomyces cerevisiae* S288c], AtPreP: NP_188548.2| presequence protease 1 [*Arabidopsis thaliana*], EcPitrilysin: NP_417298.1| protease III [*Escherichia coli* str. K-12 substrain MG1655] (characterized in Refs. 1,11,22–26, and elsewhere). All compared HsPitrm1 homologs except EcPitrilysin are members of M16C peptidase subfamily. EcPitrilysin is a member of M16A peptidase subfamily frequently referred to by the alternative identifier Protease III. Aligned sequences were presented graphically using BOXSHADE (http://www.ch.embnet.org/software/BOX_form.html), supported by the Swiss Institute of Bioinformatics. Three-dimensional structural models were based on RCSB PDB# 4NGE[8] and were generated using PyMOL (The PyMOL Molecular Graphics System, Version 1.8, Schrödinger, LLC, Cambridge, MA).

Peptide cleavage site mapping of Mca-KLVFFAEDK(Dnp)-OH

Peptide cleavage sites within the internally quenched fluorogenic Aβ-derivative substrate, Mca-KLVFFAEDK(Dnp)-OH, were mapped using MALDI-TOF. Following initiation of the kinetic assay as described above, 50 μL of a quenching solution containing 170 m*M* EDTA and 0.07% TFA were added to the assay mixture after 30 min coincubation with either WT Pitrm or mutant Pitrm R183Q. Samples were stored at −80°C until subsequent cleavage site studies were conducted. For MALDI-TOF mass spectrometry analysis of cleavage sites, 50 μL of the quenched reaction mixture was removed and the pH was adjusted to ∼pH 2 with a 0.5 μL aliquot of 10% TFA. Samples were then prepared with C_{18} Reverse-Phase ZipTip (Merck Millipore; Billerica, MA) and spotted to the MALDI plate with DHB as matrix. MALDI-TOF mass spectrometry in reflectron mode and postsource decay MS/MS of major cleavage site peptide fragments were conducted using the Shimadzu Axima Confidence mass spectrometer.

Size exclusion chromatography and multi-angle laser light scattering

SEC-MALS analysis was performed on immobilized-metal affinity chromatography purified protein

samples that were otherwise prepared as throughout this study. The light scattering data were collected using a Superdex 200, 10/300, HR Size Exclusion Chromatography (SEC) column (GE Healthcare, Piscataway, NJ), connected to high-performance liquid chromatography system (HPLC), Agilent 1200 (Agilent Technologies, Wilmington, DE). The elution from SEC was monitored by a photodiode array (PDA) UV/VIS detector (Agilent Technologies, Wilmington, DE), differential refractometer (OPTI-Lab rEx Wyatt, Santa Barbara, CA), static and dynamic, multiangle laser light scattering (LS) detector (HELEOS II with QELS capability, Wyatt, Santa Barbara, CA). The SEC-MALS analysis was performed in PBS buffer. Two software packages were used for data collection and analysis: the Chemstation software (Agilent Technologies, Wilmington, DE) controlled the HPLC operation and data collection from the multi-wavelength UV/VIS detector, while the ASTRA software (Wyatt, Santa Barbara, CA) collected data from the refractive index detector, the light scattering detectors, and recorded the UV trace at 280 nm sent from the PDA detector. The weight average molecular masses, M_w, were determined across the entire elution profile in the intervals of 1 s from static LS measurement using ASTRA software as previously described.[27]

Author Contributions

JSC synthesized, purified, and validated isolation of the Mca-KLVFFAEDK(Dnp)-OH peptide and was responsible for mapping its cleavage sites. BJA conceived this study and performed other work presented here, with the exception of SEC-MALS analysis reported in the Supporting Information. Both authors have approved the final article.

Acknowledgments

BJA thanks Walter K. Schmidt Jr. for correspondence and mentorship, and the Sacred Heart University Department of Chemistry and College of Arts and Sciences for support of this research. SEC-MALS analysis was performed by Ewa Folta-Stogniew. EFS is director of the Biophysical Resource facility operated by the Keck Foundation Biotechnology Research Laboratory at Yale University. The content of this paper is solely the responsibility of the authors and does not necessarily represent the official views of the National Institutes of Health.

Conflict of Interest

The authors of this study declare no conflicts of interest.

References

1. Mzhavia N, Berman YL, Qian Y, Yan L, Devi LA (1999) Cloning, expression, and characterization of human metalloprotease 1: a novel member of the pitrilysin family of metalloendoproteases. DNA Cell Biol 18: 369–380.
2. Becker AB, Roth RA (1992) An unusual active site identified in a family of zinc metalloendopeptidases. Proc Natl Acad Sci U S A 89:3835–3839.
3. Rawlings ND, Barrett AJ (1995) Evolutionary families of metallopeptidases. Methods Enzymol 248:183–228.
4. Falkevall A, Alikhani N, Bhushan S, Pavlov PF, Busch K, Johnson KA, Eneqvist T, Tjernberg L, Ankarcrona M, Glaser E (2006) Degradation of the amyloid beta-protein by the novel mitochondrial peptidasome, PreP. J Biol Chem 281:29096–29104.
5. Chow KM, Gakh O, Payne IC, Juliano MA, Juliano L, Isaya G, Hersh LB (2009) Mammalian pitrilysin: substrate specificity and mitochondrial targeting. Biochemistry 48:2868–2877.
6. Koscielny G, Yaikhom G, Iyer V, Meehan TF, Morgan H, Atienza-Herrero J, Blake A, Chen CK, Easty R, Di Fenza A, Fiegel T, Grifiths M, Horne A, Karp NA, Kurbatova N, Mason JC, Matthews P, Oakley DJ, Qazi A, Regnart J, Retha A, Santos LA, Sneddon DJ, Warren J, Westerberg H, Wilson RJ, Melvin DG, Smedley D, Brown SD, Flicek P, Skarnes WC, Mallon AM, Parkinson H (2014) The International Mouse Phenotyping Consortium Web Portal, a unified point of access for knockout mice and related phenotyping data. Nucleic Acids Res 42:D802–D809.
7. Johnson KA, Bhushan S, Ståhl A, Hallberg BM, Frohn A, Glaser E, Eneqvist T (2006) The closed structure of presequence protease PreP forms a unique 10,000 Angstroms^3 chamber for proteolysis. EMBO J 25:1977–1986.
8. King JV, Liang WG, Scherpelz KP, Schilling AB, Meredith SC, Tang WJ (2014) Molecular basis of substrate recognition and degradation by human presequence protease. Structure 22:996–1007.
9. Alikhani N, Guo L, Yan S, Du H, Pinho CM, Chen JX, Glaser E, Yan SS (2011) Decreased proteolytic activity of the mitochondrial amyloid-β degrading enzyme, PreP peptidasome, in Alzheimer's disease brain mitochondria. J Alzheimers Dis 27:75–87.
10. Pinho CM, Björk BF, Alikhani N, Bäckman HG, Eneqvist T, Fratiglioni L, Glaser E, Graff C (2010) Genetic and biochemical studies of SNPs of the mitochondrial A beta-degrading protease, hPreP. Neurosci Lett 469:204–208.
11. Brunetti D, Torsvik J, Dallabona C, Teixeira P, Sztromwasser P, Fernandez-Vizarra E, Cerutti R, Reyes A, Preziuso C, D'Amati G, Baruffini E, Goffrini P, Viscomi C, Ferrero I, Boman H, Telstad W, Johansson S, Glaser E, Knappskog PM, Zeviani M, Bindoff LA (2016) Defective PITRM1 mitochondrial peptidase is associated with Aβ amyloidotic neurodegeneration. EMBO Mol Med 8:176–190.
12. Maskos K, Jozic D, Fernandez-Catalan C (2005) Crystal Structure of pitrilysin, the prototype of insulin-degrading enzymes. RCSB PDB 1Q2L.
13. Shen Y, Joachimiak A, Rosner MR, Tang WJ (2006) Structures of human insulin-degrading enzyme reveal a new substrate recognition mechanism. Nature 443: 870–874.
14. Taylor AB, Smith BS, Kitada S, Kojima K, Miyaura H, Otwinowski Z, Ito A, Deisenhofer J (2001) Crystal structures of mitochondrial processing peptidase reveal the mode for specific cleavage of import signal sequences. Structure 9:615–625.
15. Teixeira PF, Pinho CM, Branca RM, Lehtiö J, Levine RL, Glaser E (2012) In vitro oxidative inactivation of

human presequence protease (hPreP). Free Radic Biol Med 53:2188–2195.
16. Mammalian Gene Collection Program Team (2002) Generation and initial analysis of more than 15,000 full-length human and mouse cDNA sequences. Proc Natl Acad Sci U S A 99:16899–16903.
17. Mammalian Gene Collection Program Team (2009) The completion of the Mammalian Gene Collection (MGC). Genome Res 19:2324–2333.
18. Candiano G, Bruschi M, Musante L, Santucci L, Ghiggeri GM, Carnemolla B, Orecchia P, Zardi L, Righetti PG (2004) Blue silver: a very sensitive colloidal Coomassie G-250 staining for proteome analysis. Electrophoresis 25:1327–1333.
19. Sievers F, Wilm A, Dineen D, Gibson TJ, Karplus K, Li W, Lopez R, McWilliam H, Remmert M, Söding J, Thompson JD, Higgins DG (2011) Fast, scalable generation of high-quality protein multiple sequence alignments using Clustal Omega. Mol Syst Biol 7:539.
20. Li W, Cowley A, Uludag M, Gur T, McWilliam H, Squizzato S, Park YM, Buso N, Lopez R (2015) The EMBL-EBI bioinformatics web and programmatic tools framework. Nucleic Acids Res 43:W580–W584.
21. McWilliam H, Li W, Uludag M, Squizzato S, Park YM, Buso N, Cowley AP, Lopez R (2013) Analysis Tool Web Services from the EMBL-EBI. Nucleic Acids Res 41: W597–W600.
22. Adams MD (2000) The genome sequence of *Drosophila melanogaster*. Science 287:2185–2195.
23. Moberg P, Ståhl A, Bhushan S, Wright SJ, Eriksson A, Bruce BD, Glaser E (2003) Characterization of a novel zinc metalloprotease involved in degrading targeting peptides in mitochondria and chloroplasts. Plant J 36: 616–628.
24. Jønson L, Rehfeld JF, Johnsen AH (2004) Enhanced peptide secretion by gene disruption of CYM1, a novel protease in *Saccharomyces cerevisiae*. Eur J Biochem 271:4788–4797.
25. Dykstra CC, Kushner SR (1985) Physical characterization of the cloned protease III gene from *Escherichia coli* K-12. J Bacteriol 163:1055–1059.
26. Finch PW, Wilson RE, Brown K, Hickson ID, Emmerson PT (1986) Complete nucleotide sequence of the *Escherichia coli* ptr gene encoding protease III. Nucleic Acids Res 14:7695–7703.
27. Folta-Stogniew E, Williams KR (1999) Determination of molecular masses of proteins in solution: implementation of an HPLC size exclusion chromatography and laser light scattering service in a core laboratory. J Biomol Tech 10:51–63.